Bioinsp. Biomim. **3** (2008) 046005 (9pp) doi:10.1088/1748-3182/3/4/046005

Bristled shark skin: a microgeometry for boundary layer control?

A W Lang[1], P Motta[2], P Hidalgo[1] and M Westcott[1]

[1] Aerospace Engineering & Mechanics Department, University of Alabama, Box 870280, Tuscaloosa, AL 35487, USA
[2] Biology Department, University of South Florida, 4202 East Fowler Avenue, Tampa, FL 33620, USA

E-mail: alang@eng.ua.edu

Received 18 January 2008
Accepted for publication 2 September 2008
Published 7 October 2008
Online at stacks.iop.org/BB/3/046005

Abstract
There exists evidence that some fast-swimming shark species may have the ability to bristle their scales during fast swimming. Experimental work using a water tunnel facility has been performed to investigate the flow field over and within a bristled shark skin model submerged within a boundary layer to deduce the possible boundary layer control mechanisms being used by these fast-swimming sharks. Fluorescent dye flow visualization provides evidence of the formation of embedded cavity vortices within the scales. Digital particle image velocimetry (DPIV) data, used to evaluate the cavity vortex formation and boundary layer characteristics close to the surface, indicate increased momentum in the slip layer forming above the scales. This increase in flow velocity close to the shark's skin is indicative of boundary layer control mechanisms leading to separation control and possibly transition delay for the bristled shark skin microgeometry.

(Some figures in this article are in colour only in the electronic version)

1. Introduction

An animal swimming through a fluid experiences three types of drag that impedes its passage. These include (i) form drag due to a difference in pressure around the body, (ii) drag-due-to-lift, and (iii) skin friction due to boundary layer formation (Bushnell and Moore 1991). At low Reynolds numbers (*Re*, based on the length of the animal in this case) skin friction predominates, while at higher *Re* pressure drag can dominate if not minimized. Drag-due-to-lift, or induced drag, is associated with the generation of longitudinal tip vortices formed primarily from the thrust producing caudal fin and is often grouped together with form drag with the summation referred to as pressure drag (Kundu and Cohen 2004). Figure 1 exhibits the estimated distribution of drag depending on whether the flow remains attached or separated around the body, where flow separation is the determining factor in high-pressure drag. It is not surprising then to consider the fact that aquatic organisms have evolved form and structures to minimize drag (Fish 1998), with the primary decrease coming from a streamlined body shape to reduce flow separation.

The skin of elasmobranch fishes (sharks, skates and rays) is covered by minute placoid scales, also called dermal denticles. The base of these bony scales is embedded in the deeper collagenous layer of the skin (dermis) termed the stratum compactum, with the crown exposed to the water. The scales over most of the body of fast-swimming sharks are particularly small (0.2–0.5 mm), have very fine and regularly spaced (30–100 μm) longitudinal ridges (similar to riblets, but discretely separated over the whole body), and are regularly aligned along the axis of the body. These minute scales can vary in size and shape with placement on the body of the shark as well as with shark species as shown in figure 2 (Bechert *et al* 2000a, 2000b, Reif 1982, 1985a, 1987). In contrast to the scales over most of the body, those on the leading edges of the body (rostrum) and fins are more firmly embedded in the skin and completely smooth (Reif 1985b, Bechert *et al* 1986). Previous studies have observed that the body scales of some fast-swimming sharks are moveable to the touch to fairly large angles on dead specimens. Such pliable, 'hand-like' scales (figure 3) have been identified over almost the entire body on the shortfin mako *Isurus oxyrinchus*

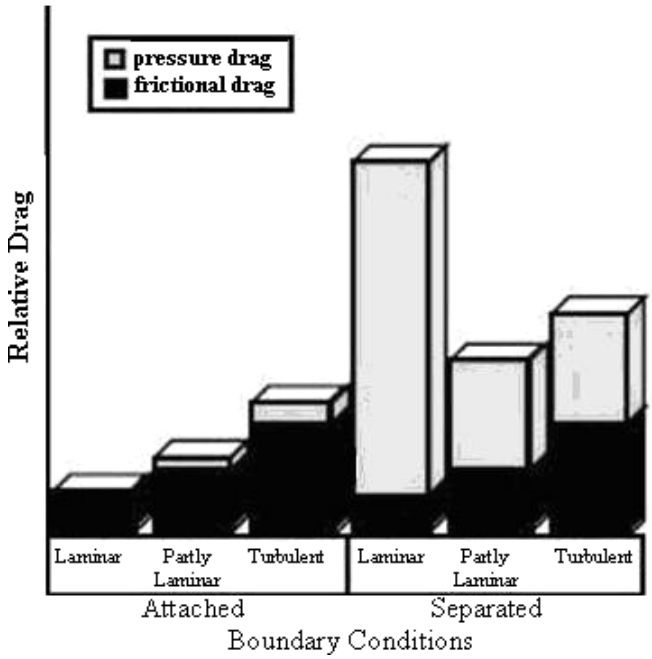

Figure 1. Relative drag associated with boundary conditions for swimming (reproduced with permission from Fish (1998)).

and smooth hammerhead *Sphyrna zygaena* (Bechert *et al* 1986).

Sharks may have the ability to bristle their scales at higher swimming speeds, or the scales might erect by passive means during high-speed swimming. The stratum compactum of sharks is composed of multiple layers of helically wound collagen fibers that form a whole body exoskeleton. These fibers, to which the base of each scale is attached, form an angle to the longitudinal axis of the shark of approximately 50–60°. This arrangement results in a balancing of longitudinal and hoop stresses in pressurized cylinders, permits bending flexibility, and results in elastic energy storage during swimming (Motta 1977, Wainwright *et al* 1978, Hebrank 1980). The erectile scales of sharks have relatively small bases, and are believed to be weakly anchored by elastic connective tissue, rather than non-elastic collagen fibers, although thorough histological analyses are lacking (Bechert *et al* 1985, Raschi and Tabit 1992). Scale erection may be accomplished through increased overall skin tension at higher swimming speeds, as the subcutaneous pressure has been demonstrated to increase from 7–14 Pa in a resting lemon shark *Negaprion brevirostris* to 200 kPa (29 psi) during fast swimming (Wainwright *et al* 1978). The change in pressure could change the helical orientation of the collagen bundles to which the scales are attached, thereby erecting the scales. On the other hand, a reduction in pressure over the loosely embedded scales could allow flow-induced bristling, possibly in adverse pressure gradient conditions where the flow is increasing in the streamline direction due to body curvature. Another possibility is that scales may bristle on regions where concave body curvature results during swimming, as these would be areas most prone to separation.

Several theories have been proposed as to the boundary layer control mechanisms of the shark skin, but to date only one has been fully tested. If the scales remain flat, the ridges on the face of each scale protrude into the flow, thereby acting as riblets, which are known to result in turbulent skin friction reduction. Man-made riblets have been experimentally shown to result in as high as a 9.9% reduction in skin friction drag (Bechert *et al* 1997). Van der Hoeven (2000) performed high-resolution DPIV measurements over riblet surfaces, and found that the cross-flow fluctuations in the turbulence close to the wall were hampered by the presence of the skin friction drag-reducing streamwise grooves. However, tests on a modeled shark skin with overlapping scales resulted in only a 3% reduction in turbulent skin friction drag (Bechert *et al* 2000a, 2000b). While there still exists debate as to the dominant source of drag on swimming sharks (skin friction may be negligible compared to pressure drag and induced drag), the above mechanism may not be the only means of reducing drag. Bechert *et al* (2000a, 2000b) attempted to consider the bristling of their shark scale model but only with respect to benefits received toward turbulent skin friction reduction at very small angles of bristling (12° or less). Possible other boundary layer control mechanisms, particularly those relating to separation control, remain untested. It should however be noted that some have hypothesized the use of bristled scales as vortex generators acting at the surface to delay flow separation and reduce pressure drag (Bechert *et al* 1985, 2000a, 2000b).

This work examines the role that scale bristling may play in controlling the boundary layer. Specifically a bristled shark skin model is tested in a water tunnel facility under both laminar and turbulent flow conditions. We also report rudimentary biological results relating to the shark skin. We present the first preliminary evidence verifying the ability of scales of two fast-swimming sharks to passively erect, and the first evidence of scale erection due to an increase in subcutaneous pressure in fresh dead specimens. Future research is planned to carry out more thorough and quantitative scientific biological studies, but the photographic evidence herein presented is of specific interest to the water tunnel studies that it warrants inclusion in this work.

2. Experimental methods

2.1. Preliminary biological manipulations

In order to validate the premise of Bechert *et al* (1986) that scales of fast-swimming sharks can be erected manually, two manipulation experiments were conducted on readily available fresh dead specimens of one specimen each of a 399 cm total length female great hammerhead shark *Sphyrna mokarran* and a 150 cm TL male blacktip shark *Carcharhinus limbatus* (Compagno 2005). Scales and attached skin anterior to the first dorsal fin was surgically removed, and the scales manipulated with a fine probe to verify that the individual scales can be erected manually. Photographs of erect scales in the sagittal plane were taken through a Meiji EMZ-5TR stereo trinocular dissecting scope (40× magnification) and an attached digital camera.

Previous studies reported that lemon sharks *Negaprion brevirostris* have subcutaneous pressures as high as 200 kPa

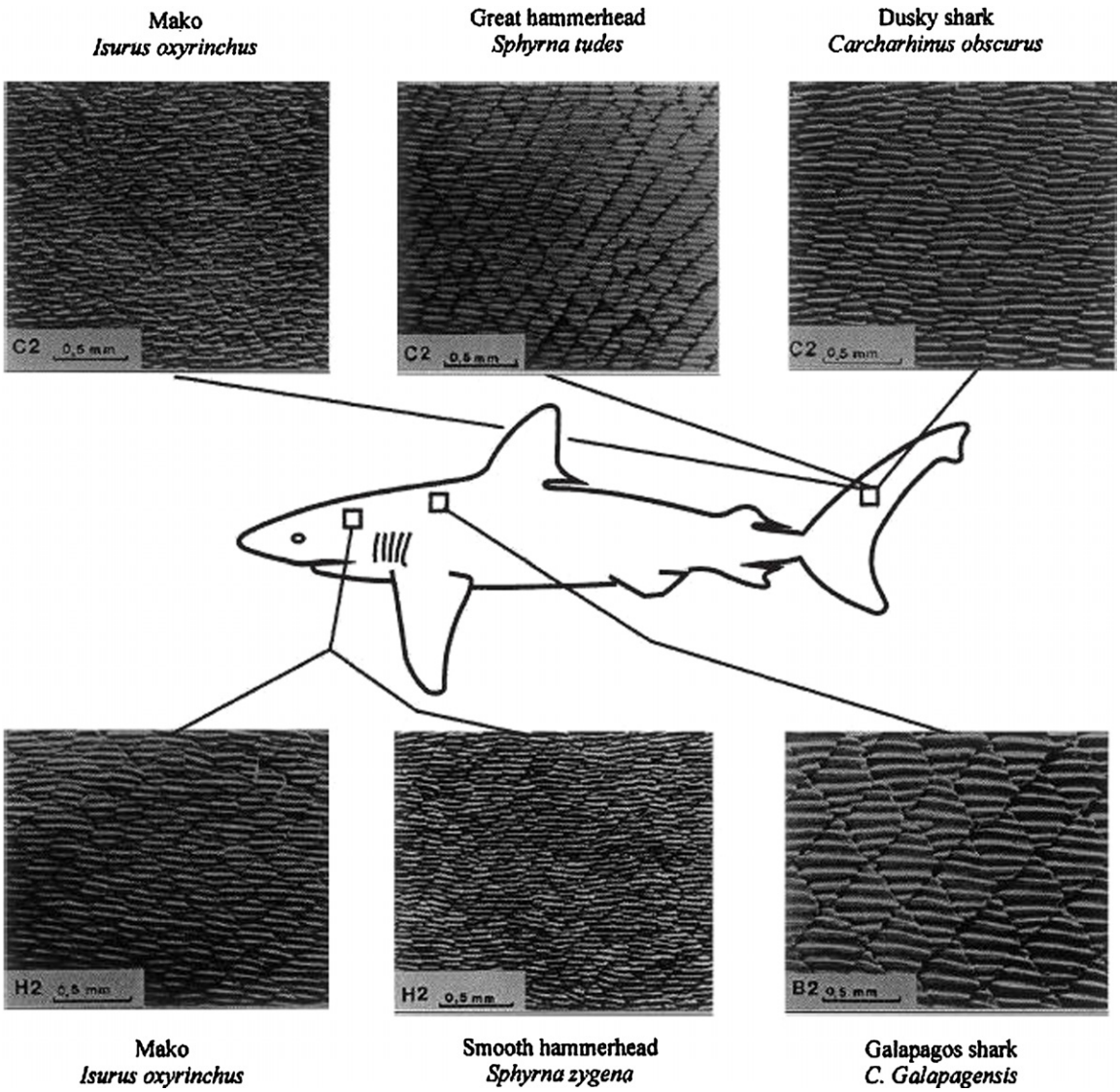

Figure 2. Scale patterns of various species of fast sharks. Reproduced with permission by Springer from Bechert *et al* (2000a, 2000b) with scale images originally obtained by Reif (1985a, 1985b).

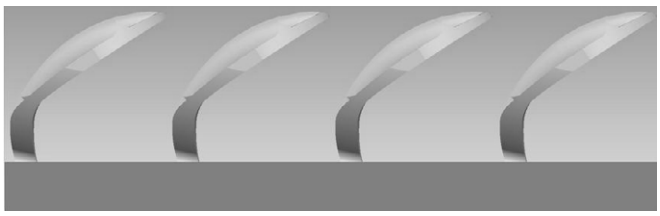

Figure 3. 'Hand'-like scales at approximate angle of bristling as that observed on dead sharks. This model was drawn using Pro-E to closely resemble the scales drawn by hand in Bechert *et al* (1985).

when swimming (Wainwright *et al* 1978). To investigate the possibility of scale erection with increase in subcutaneous pressure, a 24 French 30 cc Foley catheter was inserted through a small incision deep to the skin and superficial to the muscle just anterior and lateral to the first dorsal fin and pressurized to 14 psi (97 kPa) (figure 4). Slight scale erection, noted by a widening of the inter-scale distance, occurred solely in *S. mokarran* and was digitally photographed with a Canon A570 camera. A lateral view of these erected scales was not feasible on the intact skin. All research was conducted in accordance with the University of South Florida IACUC guidelines, protocol number T3253.

2.2. Water tunnel experiments

The goal of the water tunnel experiments was to better understand the flow field associated with scale bristling, specifically the formation of a d-type rough surface pattern resulting in the formation of embedded vortices. Experiments were performed in a water tunnel facility manufactured by Rolling Hills Research Corporation, which has a 38 cm wide by 76 cm tall by 2.75 m elongated test section. The facility is equipped with two pressurized dye reservoirs for flow visualization. UV fluorescent dye is illuminated with two 100 W UV lamps, and images are captured using a Nikon D50 color digital camera. Measurements were obtained using a

Figure 4. The experimental procedure used to demonstrate scale erection in *S. mokarran*. A Foley catheter (c) is attached to a syringe and implanted subcutaneously, being visible just below the skin (lower c). When 14 psi (97 kPa) is introduced subcutaneously (p) the placoid scales erect.

two-dimensional planar time-resolved digital particle image velocimetry (TR-DPIV) system. A Basler A504K high-speed camera, capable of 500 fps, allowed time-resolved measurements of the flow field. The flow was seeded with 10 μm silver-coated hollow glass spheres and then illuminated by a Quantronix Falcon 20 mJ Nd:YLF laser. Image acquisition and pulsing of the laser was controlled through LabVIEW on a computer, while post-processing of the images to obtain the velocity fields and other turbulence quantities was performed using Pixelflow software with a 32 $\times$ 32 correlation window size. The error in the DPIV technique is difficult to quantify as it is highly dependent on the local seeding at the time of measurement. However, an accepted error estimate is 5% in velocity measurements and 10% in vorticity (Willert and Gharib 1991, Huang *et al* 1997). It should be additionally stated that in all the data reported, averaging of several hundred (laminar) to several thousand (turbulent) velocity vector fields was performed. As an example, the local standard deviation of the vorticity under steady laminar conditions was 9.7% which falls very close to the assumed 10% error in vorticity assumed for DPIV measurements.

The shark skin model was designed based on adult shortfin mako *Isurus oxyrinchus* scale characteristics previously reported in the literature (Reif 1985a, 1985b, Raschi and Musick 1986). Raschi and Musik (1986) reported average scale characteristics of scale length $\sim$170 μm, scale width $\sim$140 μm, rib spacing $\sim$42 μm and rib height $\sim$8 μm for a 132 cm TL shark. Using these statistics, and the scanning electron micrograph image of a scale therein provided, the shark scale replica was rendered using Pro-E. Although these are average statistics and the modeled scales used in this experiment do not correspond to a particular body location, previous literature reported that loosely attached denticles were observed over the entire body of the shortfin mako (Bechert *et al* 1986). However, for the purpose of confirming the presence of embedded vortices forming in a bristled shark skin model, the scale statistics provided by Raschi and Musick (1986) were deemed sufficient for this study. This species was chosen based on its status as purportedly the fastest swimming species of shark (Reif 1985a, 1985b, Thorburn 2007). Using a rapid prototype machine, shortfin mako scales forming a 16 $\times$ 24 array were scaled up from 0.2 mm on the shark to 20 mm for the model (figure 5). With no exact data with respect to angle of bristling reported in the literature prior to this testing, an extreme angle of bristling (crown angle nearly perpendicular to the skin) was chosen for the initial study based on increased optical access to the cavities for flow measurement and maximum cavity opening conducive to the formation of embedded vortices. Further studies are planned for variation in angle of bristling, but only data for this extreme angle are reported here. In addition, to simplify the experimental conditions and model construction, the scales were fixed in position as the purpose was to study the cavity vortex formation inside a bristled shark skin geometry.

Reynold's Number (Re) can be defined based on the length of a shark's body ($Re \sim 10^7$) which would signify turbulent flow, or on denticle crown length (d), resulting in a more localized Re. Similarity of the cavity flow was achieved by matching the localized $Re \sim 2800$ of the shark skin and the model (the scale up in size is countered by a scale down in velocity over the surface from approximately 20 m s^{-1} to 20 cm s^{-1} with slight change in viscosity). It is this localized Re which is matched in the water tunnel experiments to

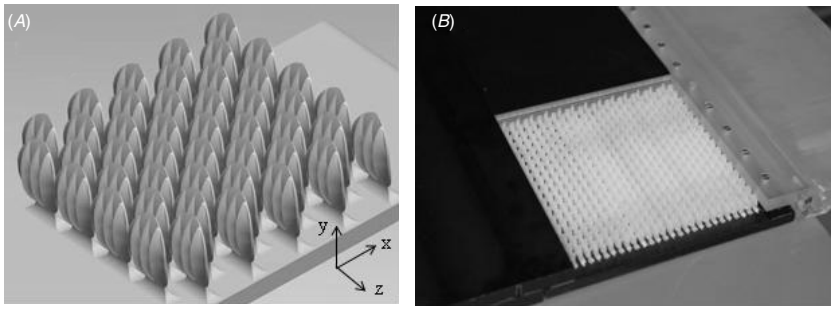

Figure 5. Bristled shark skin model. (*A*) Pro-E rendering. (*B*) Model built for water tunnel testing with shark skin embedded into the flat plate model.

achieve flow similarity, such that the boundary layer thickness to denticle crown ratio (δ/d) is sufficiently large enough such that it is comparable to values found above the shark skin. However, both laminar and turbulent boundary layer conditions are tested as on the fins, in particular, laminar or transitioning flow may be present on some areas of the shark skin. This is particularly true if transition delay mechanisms, such as a favorable pressure gradient or riblets (Choi 2000, Grek *et al* 1995), are working to delay the point of transition.

A long flat plate (∼90 cm) with an elliptic leading edge (Fransson 2004) was used to grow the boundary layer sufficiently thick such that shear layer instabilities over the cavity vortices were not observed to develop. In the case of the shark skin, this boundary layer growth occurs over the smooth scales found at the nose and fin leading edges. The model was also embedded into the plate such that only the top 1.25 mm of the tips protruded into the boundary layer flow. This protrusion has the purpose to create a momentum balance between the blockage due to the protruding tips and the flow going through the valleys between peaks, which would otherwise tend to have a downward motion into the cavities. Data were obtained for various cross-sections with respect to various x–y planes, where a separation of 15.6 mm exists between scale peaks in each row and a separation of half that distance or 7.8 mm between peaks of staggered rows

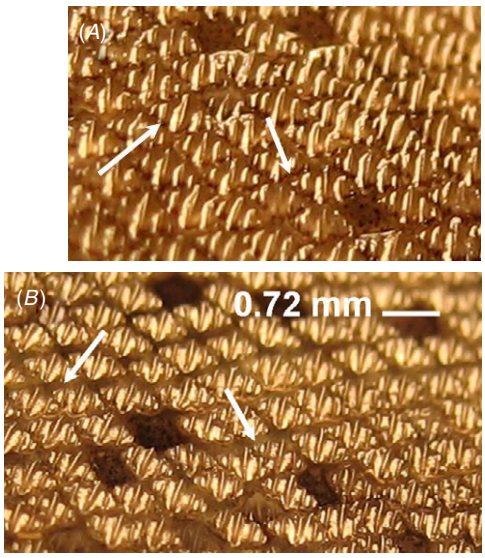

Figure 6. Placoid scales of *S. mokarran* before (*A*) and after (*B*) subcutaneous pressure. The space between individual scales is restricted as each scale abuts the adjacent scales (arrows). After 14 psi is introduced the scales erect resulting in a larger space between adjacent scales (arrows) and a more bristled appearance to the skin. Each scale is approximately 0.72 mm from lateral edge to edge. The small pores on the skin are superficial neuromasts, which are sensory receptors.

3. Results

3.1. Biological experiments

The first rudimentary experimental photographic evidence of a mechanism for scale bristling in some fast-swimming sharks is reported. These results are preliminary, and future quantitative work is planned. The scales were observed to erect when the skin was pressurized on *S. mokarran* resulting in an increase in the inter-scalar distance, giving the skin a bristled appearance (figure 6(*B*)). Upon release of pressure the scales returned to their normal position with their lateral margins almost touching each other (figure 6(*A*)). Before and after pressure application the scales remained relatively loosely attached, demonstrated no apparent erection, yet under both conditions were able to be manually erected (by a fine probe) to approximately 30° to the skin's surface (figure 7). Upon release, they returned to their normal horizontal position. Additionally, manual manipulation of the scales on *C. limbatus* was also performed, and again a fairly large angle was easily obtained with very little force applied by the fine probe to the scale. Bristling angles in the range of 30–40° were observed (figure 8). Subcutaneous pressure application did not result in any apparent scale erection in *C. limbatus* despite being repeated on adjacent areas anterior to the first dorsal fin.

3.2. Water tunnel experiments

First, fluorescent dye was used to visualize of the flow over the bristled shark skin model, revealing the formation of embedded cavity vortices (figure 9). One can initially visualize that the flow appears to skip over the surface, and that the flow is not immediately tripped to a turbulent state by this rough

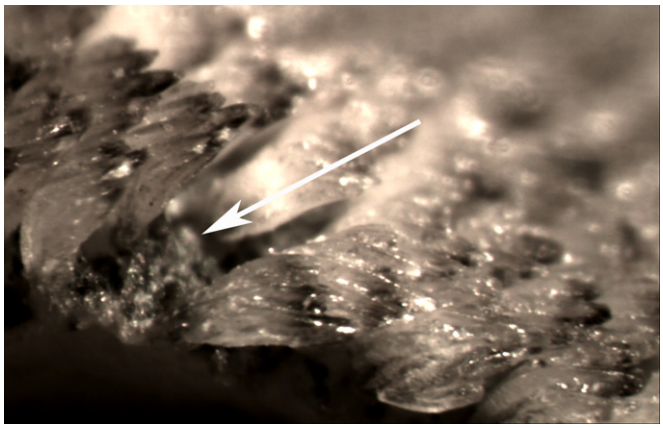

Figure 7. A sagittal section through the skin and scales of a *S. mokarran* anterior to the first dorsal fin with the scales to the left manually erected by a probe. Anterior is to the left. The scales to the right are in the resting anatomical position and the arrow indicates the cavity formed between the erected and non-erected scales, which is slightly exaggerated in size due to the abutment of erect and non-erect scales.

surface embedded into the boundary layer. The primary vortex formation within the surface appears to be confined to the upper half of the cavity formed by the bristled scales.

Figures 10(*A*) and (*B*) show views from the side of the model with velocity data confirming the formation of the primary cavity vortex, visualized in the fluorescent dye studies, with a free stream velocity of 20 cm s^{-1}. DPIV measurements reveal an interlocking web of vorticity embedded within the scale surface, with the strongest vorticity forming in front of each scale peak, as visualized in figure 9. To measure the formation of secondary vorticity, measurements were also

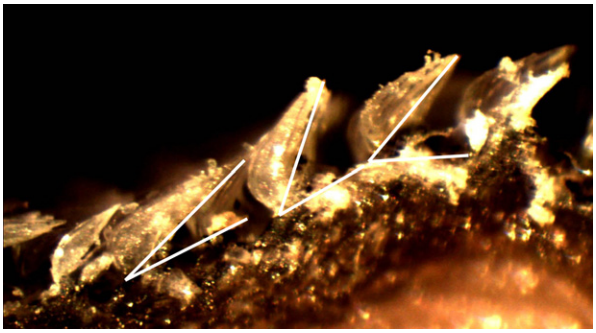

Figure 8. A sagittal section through the skin and scales anterior to the first dorsal fin of a blacktip shark *C. limbatus*. Anterior is towards the left. The scales have been manually manipulated by a probe so that the three scales towards the right have erected to greater than 30°, whereas the scale on the extreme left is in the resting position. The picture was taken with a dissecting microscope at 40× magnification and an in-line digital camera.

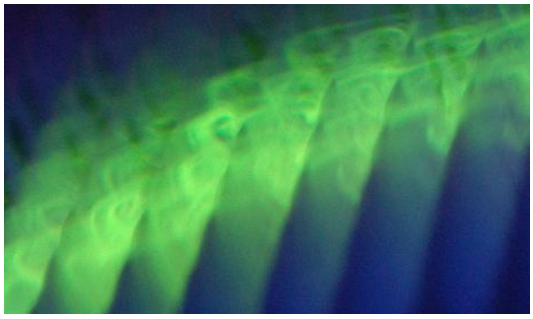

Figure 9. Green fluorescent dye visualizes embedded vortices forming in the surface(scales are bluish black in color). Flow passes left to right.

taken for various x–z planes, in particular, the plane at 0% and 20% cavity depth is shown in figure 11. There exist counter-rotating pairs of vortices forming between the three ribs, and the ribs appear to promote the formation of this secondary vorticity while additionally preventing the flow from passing around the sides of the tips, thereby also increasing the strength of the primary cavity vortex. Velocity data from the x–z plane at $y = 0$ (e.g., figure 11(*A*)) were analyzed to find the peak slip velocities along the surface and to calculate an average velocity in this plane for the surface. Peak velocities ranged on the order of 2.78 cm s^{-1} or roughly 14% of the freestream velocity. Averaged velocity for the $y = 0$ plane, again under laminar flow conditions, was 0.54 cm s^{-1} or 3% of the freestream velocity. These values are in comparison to a flat, smooth surface which at $y = 0$ results in a zero velocity due to the no-slip condition.

Turbulent boundary layer conditions were also measured to discern the on average cavity flow field by tripping the boundary layer prior to passing over the model. In this case, time-resolved DPIV images of the flow revealed sporadic events of fluid influx/efflux driven into/out of the cavities by the turbulent flow fluctuations occurring in the boundary layer above, as was expected. The additional fact that, on average, a turbulent boundary layer has higher momentum closer to the surface, resulted in much higher momentum occurring on average above and within the cavities as well (figure 12). A primary vortex is still present on average, but it is located deeper inside the cavity and is slightly reduced in size. The peak velocities increased to 28% (5.6 cm s^{-1}) and the averaged velocity in the $y = 0$ plane also increased to 10% (2 cm s^{-1}) of the freestream flow; these increases were expected for turbulent boundary layer conditions. The turbulent cavity vortex flow field on average also resembled that found under laminar conditions (figure 13), just embedded

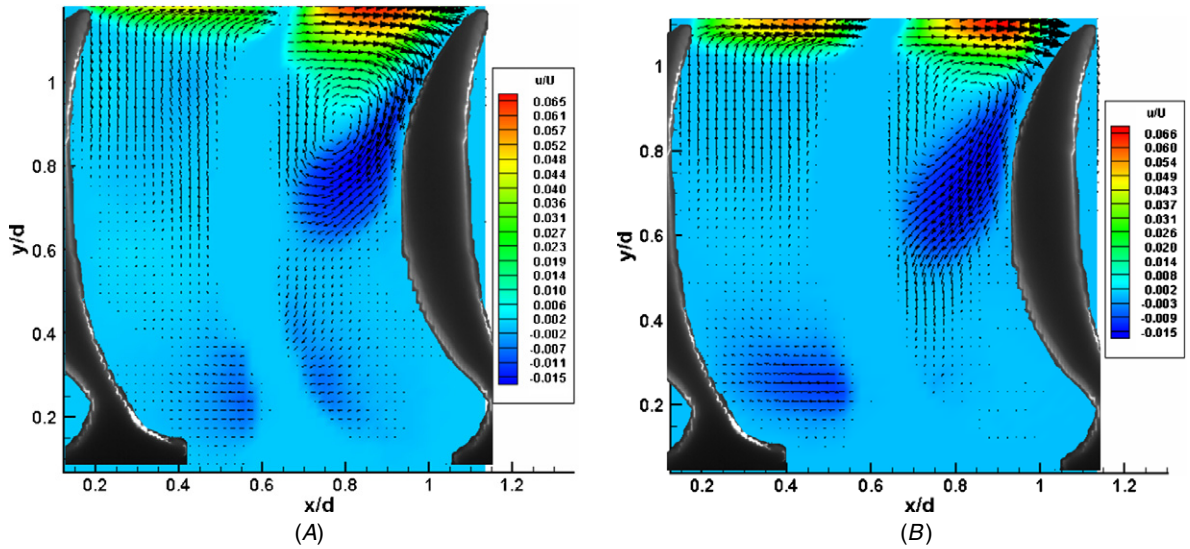

Figure 10. (*A*) Laminar flow velocity field between peaks in the denticle model showing the formation of an embedded vortex within the cavity between two denticles peaks. Note blockage from the middle row of denticles gives no data in the denticle shaped area (the flow is passing through a valley between peaks of this middle row in this plane). To left and right is shown a side profile of the bristled denticles (peaks in this plane). (*B*) Same view at a different cross-section located 4 mm behind the view shown in *A*. This location corresponds to a mid-distance between an upstream and downstream peak, and 25% of the distance towards an adjacent peak. The primary cavity vortex is still evident.

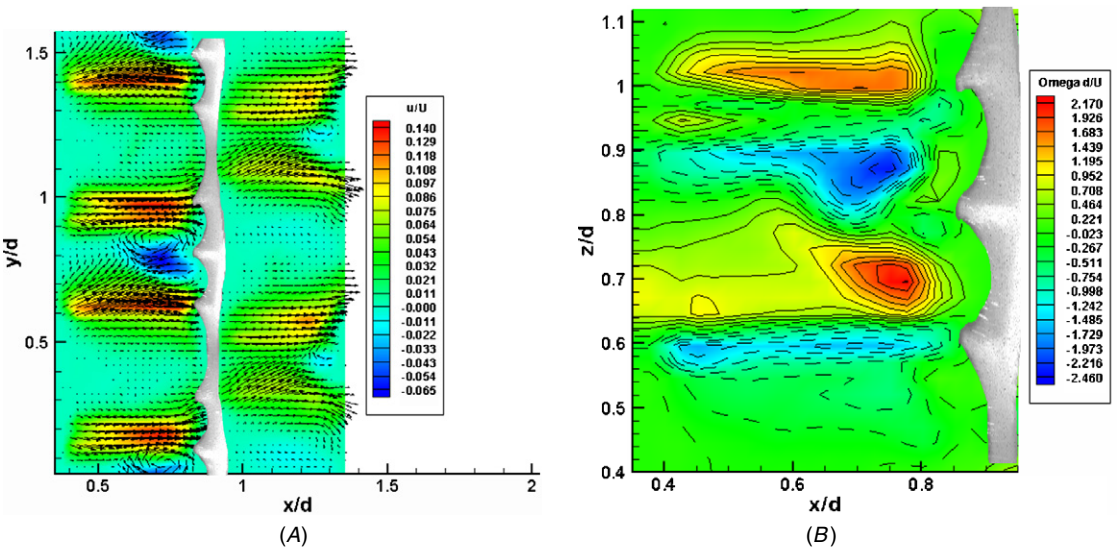

Figure 11. (*A*) Laminar flow velocity fields (top view: looking down into the space between denticles) at 0% cavity depth displaying the partial slip pattern induced at the $y = 0$ plane. (*B*) Laminar flow vorticity field at 20% cavity depth (zoomed in view showing the formation of secondary and tertiary vortices). Dorsal side of denticle with riblets produces higher order vorticity, due to downward flow of the primary vortex close to the denticle surface, as shown at the right of the image.

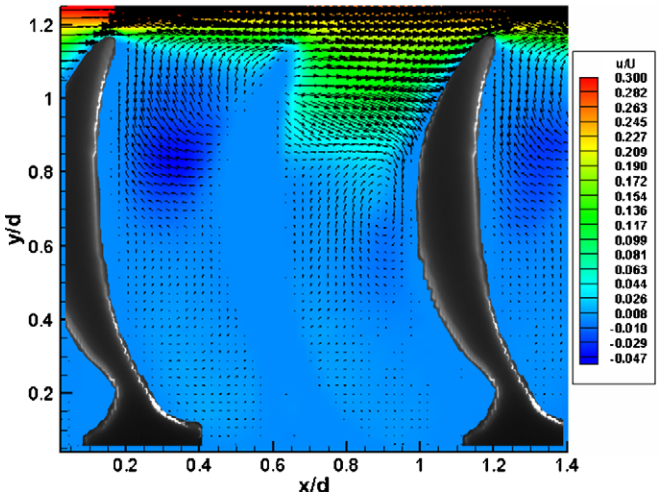

Figure 12. Averaged turbulent cavity flow velocity field between peaks in the denticle model. Flow passes left to right in all images.

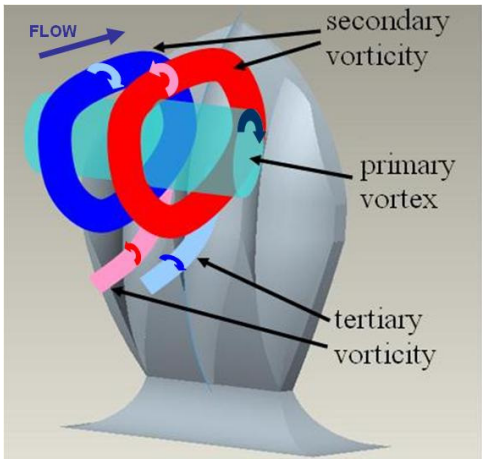

Figure 13. Schematic of vorticity forming in the embedded cavity created by bristled shark skin denticles on the dorsal(anterior) side of one scale. Red and blue coloring designates positive and negative vorticity, respectively, consistent with figure 10(*B*).

slightly deeper into the cavity and of slightly smaller size but higher strength. These initial results point to higher momentum in the $y = 0$ plane for the bristled shark skin model, compared to a flat surface which by the no-slip condition would have zero momentum in the $y = 0$ plane for both laminar and turbulent boundary layer conditions.

4. Discussion

Scales of fast-swimming sharks have been implicated in drag reduction (Raschi and Tabit 1992, Reif 1982, 1985a) and preliminary work on models with semi-erect scales has resulted in minimal drag reduction (Bechert *et al* 2000a, 2000b). Key to the theoretical predictions is the ability of the scales to erect (Bechert *et al* 1985, 1986, 2000a, 2000b), either actively or passively, and the formation of embedded vortices between adjacent scales. Our preliminary findings indicate that erection of scales of at least two fast-swimming species is feasible, in consonance with the observations on other species by Bechert *et al* (1986). In addition, we found erection to possibly occur due to both a subcutaneous increase in pressure on *S. mokarran*, while on both species the scales were easily moveable to the touch to angles in excess of 30°. Experiments modeling an extreme angle of bristling for shortfin mako denticles confirmed the formation of embedded vortices within the inter-denticular cavities.

While a single shark scale immersed in a boundary layer may result in the scale looking and acting as a vortex generator, when working together as an array of scales the experimental evidence presented substantiates an entirely different effect. This flow phenomenon is similar to the difference between *k*-type roughness and d-type roughness as described by

Jimenez (2004), where k is defined as the height of the roughness protrusion. When spacing between roughness elements is less than 3–4 k, flow over the surface causes the formation of recirculation zones, or embedded vortices, between the protrusions and the roughness is characterized as a d-type rough surface. When spacing is greater than 3–4 k, the protrusions each form a wake independent of the closest protrusion. This larger spatial distance between protrusions would be needed to form a surface where each protrusion acted as an independent vortex generator. However, in the case of the erect shark skin, if significant bristling is present then the spatial distance is close enough to result in the formation of embedded vortices within the shark skin surface, thus resulting in a d-type surface, and this is what has been observed in this study. This primary vortex interacting with the scale face results in the formation of opposite sign vorticity in the vicinity where the flow induced by the vortex passes over the solid surface of the scale. This result is similar to that observed in square lid-driven cavity vortices (Shankar and Deshpande 2000). Furthermore, it appears that the geometry of this particular surface replicating a shark scale has the ability to promote the formation of secondary vorticity superimposed upon the primary core vortex. As these vortices form deeper inside the cavity, additional smaller tertiary vortices of opposite sign form close to the scale surface due to the interaction of the stronger secondary vorticity with the no-slip wall. This is similar in effect to the opposite sign vorticity described above, as well as to the flow phenomenon observed in the unsteady vortex/wall interaction reported by Gendrich *et al* (1997). All levels of vorticity (except the opposite sign vorticity sheet generated off the face of the scale by the primary vortex) are visualized in figure 13. For scales loosely attached to the skin the formation of this vortex in combination with an adverse streamwise pressure gradient could lead to a fluid-structure interaction (whereby low pressure upstream and above the scale causes scale bristling) as a means of separation control.

In some cases involving low Re flow over d-type roughness, embedded vortices may reduce skin friction drag through the so-called 'fluid roller bearing' effect. In this theoretical work involving a d-type sinusoidal surface, embedded vortices form resulting in a drag reduction for creeping flows (Scholle *et al* 2006, Scholle and Aksel 2006). Scholle (2007) also showed the importance of the shape of the geometry on the drag reduction potential. A more blade-like shape with thin peaks proved more conducive to the vortex filling the entire cavity, thus resulting in greater drag reduction potential under Couette flow conditions. The work reported here involves three-dimensional denticle peaks protruding into the flow, which could lead to increased localized skin friction (surface drag) over these small protuberances. But, the formation of embedded vortices allowing the fluid to skip over the cavities has the potential to contribute to global separation control. In this respect, the 'fluid roller bearing' effect attributed to a d-type roughness can have multiple uses resulting in either skin friction reduction by reducing the contact of the flow with the actual surface (fluid skips over the surface via the fluid roller bearing), and form drag reduction through separation control. However, the actual use of these surfaces to achieve either of these flow control mechanisms appears to be dependent on the Re, and is a topic of further study.

Thus, these embedded vortices, analogous to dimples acting on a golf ball, may work as a boundary layer control mechanism to passively delay, or even prevent, flow separation, thereby reducing form drag. This theory is substantiated by the measured higher momentum associated with the $y = 0$ plane, where this higher momentum is considered a positive sign toward achieving separation delay (Gad-el-Hak 2000). It should, however, also be pointed out that whereas a dimpled surface has no direction of preferred flow, the shark skin clearly does for various angles of bristling. This preferential flow direction is clearly evident in that flow reversal is inhibited by angled scales having larger skin friction drag if the boundary layer flow above the surface is reversed. Future study is planned to better understand the preferential flow direction of the bristled shark skin surface.

Finally, it is feasible that the model surface could work in a unique way to counteract the formation of instabilities found in three-dimensional boundary layers by disrupting the formation of the optimal instabilities which grow and lead to transition. Practical methods through the use of roughness elements have been shown to result in transition delay or laminar flow control (Fransson *et al* 2006, Saric *et al* 2003). Achieving greater regions of laminar flow over the shark's skin, particularly toward the front of the shark where skin friction is largest, may also contribute to reduction in overall drag (Neumann and Dinkelacker 1989) and should be considered as an additional and feasible boundary layer control mechanism.

5. Conclusions

Our preliminary analysis of the great hammerhead shark *S. mokarran* and the blacktip shark *C. limbatus* indicates that the scale erection by subcutaneous pressure may be possible and species specific. In addition, the first photographic evidence is presented that the scales of some fast-swimming sharks are pliable and may erect passively. Experimental studies of a bristled shortfin mako scale model revealed the formation of embedded vortices within the model. DPIV measurements revealed that this leads to higher momentum in the flow close to the model (partial slip at the $y = 0$ plane) as compared to a flat, smooth surface (no-slip condition) for both laminar and turbulent boundary layer conditions. Finally, it is postulated that the unique microgeometry of bristled shark skin can have the potential to result in more than one means of controlling the boundary layer to decrease overall drag.

Acknowledgments

Support for this research by a NSF SGER grant CTS-0630489, Lindbergh Foundation Grant and a University of Alabama RAC grant is gratefully acknowledged. Mr Westcott was supported as a REU student under the NSF grant. The Porter Family Foundation graciously supported the research at the University of South Florida.

References

Bechert D W, Bartenwerfer M and Hoppe G 1986 Drag reduction mechanisms derived from the shark skin *15th ICAS Congress (London, UK)* pp 1044–68

Bechert D W, Bruse M and Hage W 2000a Experiments with three-dimensional riblets as an idealized model of the shark skin *Exp. Fluids* **28** 403–12

Bechert D W, Bruse M, Hage W and Meyer R 2000b Fluid mechanics of biological surfaces and their technological application *Naturwissenschaften* **80** 157–71

Bechert D W, Bruse M, Hage W, Van der Hoeven J and Hoppe G 1997 Experiments on drag-reducing surfaces and their optimization with an adjustable geometry *J. Fluid Mech.* **338** 59–87

Bechert D W, Hoppe G and Reif W E 1985 On the drag reduction of the shark skin *AIAA Shear Flow Control Conf. Proc. (Boulder, CO, 12–14 Mar.)*

Bushnell D and Moore K 1991 Drag reduction in nature *Ann. Rev. Fluid Mech.* **23** 65–79

Choi K 2000 European drag-reduction research—recent developments and current status *Fluid Dyn. Res.* **26** 325–35

Compagno L, Dando M and Fowler S 2005 *Sharks of the World* (Princeton, NJ: Princeton University Press)

Fish F 1998 Imaginative solutions by marine organisms for drag reduction *Proc. Int. Symp. Seawater Drag Reduction* pp 1–8

Fransson J 2004 Leading edge design process using a commercial flow solver *Exp. Fluids* **37** 929–32

Fransson J, Talamelli A, Brandt L and Cossu C 2006 Delaying transition to turbulence by a passive mechanism *Phys. Rev. Lett.* **96** 064501

Gad-el-Hak M 2000 *Flow Control: Passive, Active and Reactive Flow Management* (Cambridge, UK: Cambridge University Press)

Gendrich C, Bohl D and Koochesfahani M 1997 Whole-field measurement of unsteady separation in a vortex ring/wall interaction AIAA paper 97–1780

Grek G, Kozlov V and Titarenko S 1995 The influence of riblets on a boundary layer with embedded streamwise vortices *Phys. Fluids* **7** 2504–6

Hebrank M R 1980 Mechanical properties and locomotor functions of eel skin *Biol. Bull.* **158** 58–68

Huang H, Dabiri D and Gharib M 1997 On errors of digital particle image velocimetry *Meas. Sci. Technol.* **8** 1427–40

Jimenez J 2004 Turbulent flows over rough walls *Ann. Rev. Fluid Mech.* **36** 173–96

Kundu P and Cohen I 2004 *Fluid Mechanics* (London, UK: Academic)

Motta P 1977 Anatomy and functional morphology of dermal collagen fibers in sharks *Copeia* **1977** 454–64

Neumann D and Dinkelacker A 1989 Drag reduction by longitudinal riblets on the surface of a streamwise aligned body of revolution *Drag Reduction in Fluid Flows* (Chichester, UK: Ellis Horwood)

Raschi W and Musick J 1986 Hydrodynamic aspects of shark scales *NASA Contractor Rep*. 3963

Raschi W and Tabit C 1992 Functional aspects of placoid scales: a review and update *Aust. J. Mar. Freshwater Res.* **43**123–47

Reif W E 1982 Hydrodynamics of the squamation in fast swimming sharks *N. Jb. Geol. Paläont.* **164** 184–7

Reif W E 1985a Morphology and hydrodynamic effects of the scales of fast swimming sharks *Fortschr. Zool.* **30** 483–5

Reif W E 1985b Squamation and ecology of sharks *Courier Forschungsinstitut Senckenberg* no 78 (Frankfurt am Main)

Reif W E 1987 Squamation of hammerhead sharks: variation in the polarity field *Zool. Jb. Anat.* **115** 153–61

Saric W, Reed H and White E 2003 Stability and transition of three-dimensional boundary layers *Ann. Rev. Fluid Mech.* **35** 413–40

Scholle M 2007 Hydrodynamical modelling of lubricant friction between rough surfaces *Trib. Int.* **40** 1004–11

Scholle M and Aksel N 2006 Shark skin effect in creeping films arXiv:physics/0605232

Scholle M, Rund A and Aksel N 2006 Drag reduction and improvement of material transport in creeping films *Arch. Appl. Mech.* **75** 93–112

Shankar P and Deshpande M 2000 Fluid mechanics in the driven cavity *Ann. Rev. Fluid Mech.* **32** 93–136

Thorburn C 2007 Personal communication. Video evidence available in *Animal Nation: Mako Sharks* available on DVD

Van der Hoeven J 2000 Observations in the turbulent boundary-layer–high resolution DPIV measurements over smooth and riblet surfaces *PhD Thesis* Delft University of Technology, The Netherlands

Wainwright S 1978 Shark skin: a function in locomotion *Science* **202** 747–9

Willert C and Gharib M 1991 Digital particle image velocimetry *Exp. Fluids* **10** 181–93